

YITP-SB-02-79
December 24, 2002

Interjet Energy Flow/Event Shape Correlations

Carola F. Berger¹, Tibor Kúcs, and George Sterman

*C.N. Yang Institute for Theoretical Physics, SUNY Stony Brook
Stony Brook, New York 11794 – 3840, U.S.A.*

Abstract

We identify a class of perturbatively computable measures of interjet energy flow, which can be associated with well-defined color flow at short distances. As an illustration, we calculate correlations between event shapes and the flow of energy, Q_Ω , into an interjet angular region, Ω , in high- p_T two-jet e^+e^- -annihilation events. Laplace transforms with respect to the event shapes suppress states with radiation at intermediate energy scales, so that we may compute systematically logarithms of interjet energy flow. This method provides a set of predictions on energy radiated between jets, as a function of event shape and of the choice of the region Ω in which the energy is measured. Non-global logarithms appear as corrections. We apply our method to a continuous class of event shapes.

1 Introduction

Inclusive jet cross sections have a long history, and the agreement of predictions based on perturbative QCD with experiment is often impressive. The study of energy flow into the regions between energetic jets [1] gives important, and in some sense complementary information about the formation of final states. Interjet energy flow is expected to reflect the flow of color at short distances [1, 2, 3] and may give insight into the hadronization process. In addition, knowledge of the relation between energy and color flows is important for investigating hard collisions [4], to distinguish QCD bremsstrahlung originating in the underlying hard scattering or decay from radiation induced by multiple scatterings. The study of observables in jet events that test the flow of energy is thus of considerable interest. The computation of such observables, however, has turned out to be subtle [5], for reasons that we will briefly review below. For definiteness, we will discuss these issues in dijet events at large center-of-mass energy Q in e^+e^- -annihilation [6]. In this case the underlying color flow at short distances is unique, corresponding to the creation of a quark-antiquark pair. This enables us to illustrate our method, while avoiding the complication of multiple color exchanges, for example, singlet and octet exchange in quark-antiquark scattering [2, 3].

We study the flow of energy or transverse energy, $Q_\Omega \equiv \varepsilon Q$, with $\varepsilon \ll 1$, into an interjet angular region, Ω . The process

$$e^+ + e^- \rightarrow 2 \text{ Jets} + X_{\bar{\Omega}} + R_\Omega(Q_\Omega), \quad (1)$$

is illustrated in Fig. 1. $X_{\bar{\Omega}}$ represents soft radiation into the region between Ω and the jet axes, denoted by $\bar{\Omega}$, and R_Ω denotes soft radiation into Ω . Our goal is to relate soft radiation into region Ω to the hard scattering that produces the jets.

¹Based on talk given by C. F. Berger at TH2002, Theme 2: “QCD, Hadron dynamics, etc.”, Paris, France, 2002.

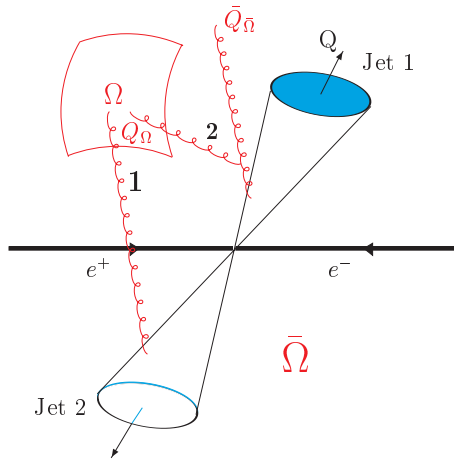


Figure 1: Sources of global and non-global logarithms in dijet events. Configuration 1, a primary emission, is the source of global logarithms, configuration 2 results in non-global logarithms.

Following [5], we refer to observables as “non-global” when they are defined by radiation into a specific portion of phase space, while remaining more-or-less inclusive elsewhere. In non-global cross sections there are two sources of logarithmic corrections, as indicated in Fig. 1: “primary” emissions, such as gluon 1 in Fig. 1, are emitted directly from the hard partons into Ω . Phase space integrals for these emissions contribute single logarithms per loop: $\alpha_s^n \ln^n(Q/Q_\Omega) = \alpha_s^n \ln^n(1/\varepsilon)$. These logarithms exponentiate, and may be resummed in a straightforward fashion [3]. There are also “secondary” emissions originating from the complementary region $\bar{\Omega}$, illustrated by configuration 2 in Fig. 1. As emphasized by Dasgupta and Salam [5], emissions into Ω from such secondary partons can give logarithms of the form $\alpha_s^n \ln^n(\bar{Q}_{\bar{\Omega}}/Q_\Omega)$, where $\bar{Q}_{\bar{\Omega}}$ is the maximum energy of radiation in $\bar{\Omega}$. These have become known as non-global logarithms. If no restriction is placed on the radiation into $\bar{\Omega}$, then $\bar{Q}_{\bar{\Omega}}$ can approach Q , and the non-global, secondary logarithms can become as important as the primary logarithms. The non-global logarithms arise because real and virtual enhancements associated with secondary emissions do not cancel each other fully at fixed Q_Ω . In general, such non-global logarithms, as studied in [5] and [7], are sensitive to color flow at all scales and in all directions, and they do not exponentiate in the same simple manner as do logarithmic enhancements from primary emission. In a sense, they mask the underlying color exchange at short distances.

In the studies of non-global observables in Refs. [5, 7], numerical estimates of both types of logarithms were carried out in various situations. Here we will adopt a somewhat different strategy, and introduce correlations between energy flow and event shapes (“flow/shape correlations”). Our aim is to select final states whose formation is sensitive primarily to radiation from the highest-energy jets. By restricting the range of event shapes, we can systematically limit radiation in region $\bar{\Omega}$ while retaining the chosen jet structure. This allows us to treat all leading effects analytically. In essence, the color and energy flow originating from the primary radiation is less obstructed by secondary radiation. Our approach does not resum non-global logarithms, but allows us to address the question of interjet energy flow within a more global context, while retaining the original motivation and physical picture described above.

2 Energy Flow/Event Shape Correlations

The following observation allows us to avoid leading contributions from non-global configurations such as gluon 2 in Fig. 1. Large non-global logarithms originate from emissions into $\bar{\Omega}$ at relatively large angles from the jets, because radiation from partons close to the jet directions is emitted coherently. By fixing the value of an event shape near the two-jet limit, we avoid final states with large energies in $\bar{\Omega}$ at fixed angles from the jet axes. To impose this two-jet condition at fixed energy flow, we will introduce shape functions \bar{f}_c , $c = 1, 2$, one for each jet, for radiation into $\bar{\Omega}$. The relevant cross section for the process (1), at fixed direction for jet 1, \hat{n}_1 , is then defined as

$$\begin{aligned} \frac{d\bar{\sigma}(\varepsilon, \bar{\varepsilon})}{d\varepsilon d\bar{\varepsilon} d\hat{n}_1} &= \frac{1}{2Q^2} \sum_N |M(N)|^2 (2\pi)^4 \delta^4(p_I - p_N) \\ &\times \delta(\varepsilon - f(N)) \delta(\bar{\varepsilon} - \bar{f}_1(N) - \bar{f}_2(N)) \delta(\hat{n}_1 - \hat{n}(N)), \end{aligned} \quad (2)$$

with the energy flow fixed by

$$f(N) = \frac{1}{Q} \sum_{\hat{n}_i \in \Omega} \omega_i. \quad (3)$$

We sum over all final states N that contribute to the weighted event, with $M(N)$ the amplitude for $e^+e^- \rightarrow N$. The total momentum is p_I , with $p_I^2 \equiv Q^2$. To define the total event shape $\bar{\varepsilon}$ in Eq. (2) we divide $\bar{\Omega}$ into two hemispheres, each surrounding one of the jets. Each hemisphere contributes separately, through \bar{f}_1 and \bar{f}_2 . An example of a suitable shape function is the thrust-like weight

$$\bar{f}_c(N) = \frac{1}{Q} \sum_{\hat{n}_i \in \bar{\Omega}_c} \omega_i (1 - \cos \theta_i), \quad c = 1, 2, \quad (4)$$

where θ_i are the angles with respect to the jet directions. The cross section Eq. (2) measures the correlation of $\bar{\varepsilon} = \bar{f}_1 + \bar{f}_2$ with the energy flow into Ω . Since we are interested in two-jet cross sections, we fix the constants ε and $\bar{\varepsilon}$ to be much less than unity:

$$0 < \varepsilon, \bar{\varepsilon} \ll 1. \quad (5)$$

In this limit, we can neglect recoil due to the soft radiation. Generalizations to more than two jets in the final state, and to correlations with transverse energy flow into Ω , are clearly possible.

In the limit (5) the cross section (2) has large logarithmic enhancements in $\ln 1/\varepsilon$ and $\ln 1/\bar{\varepsilon}$, which we will resum. However, we will not resum logarithms like $\ln(\bar{\varepsilon}/\varepsilon)$. Instead, the following generalization of Eq. (4) to the weights $\bar{f}_c(N, a)$ allows us to study correlations of jet structure with energy flow into Ω :

$$\bar{f}_c(N, a) = \frac{1}{Q} \sum_{\hat{n}_i \in \bar{\Omega}_c} \omega_i \sin^a \theta_i (1 - \cos \theta_i)^{1-a}, \quad c = 1, 2, \quad a < 2. \quad (6)$$

As $a \rightarrow 2$ the weight vanishes only very slowly for $\theta_i \rightarrow 0$, and at fixed \bar{f}_c , the jet becomes very narrow. On the other hand, as $a \rightarrow -\infty$, the event shape vanishes in nearly every direction, and the cross section at fixed \bar{f}_c becomes more and more inclusive in radiation into $\bar{\Omega}$. In this limit, non-global logarithms reemerge as leading effects. For $a = 0$ we obtain the thrustlike weight (4) discussed above;

the case $a = 1$ corresponds to the jet broadening. The effect of a on the shape of the radiation into $\bar{\Omega}$ is illustrated in Fig. 2. In Fig. 2 we compare the phase space available to a particle at fixed $\bar{\varepsilon}$ for three different values of a . The radial magnitude of each plot is the maximum energy ω found from Eq. (6): $r = \bar{\varepsilon}Q \sin^{-a} \theta (1 - \cos \theta)^{a-1}$. For $a = 1$, as shown in Fig. 2 a), the particle is restricted to be close to the jet axes, while for $a = 0$, and $a = -1$, depicted in Figs. 2 b) and c), respectively, the particle is allowed to be farther away from the axes. With the above choices of weight functions the cross section (2) is infrared safe, and logarithms of ε and $\bar{\varepsilon}$ may be resummed.

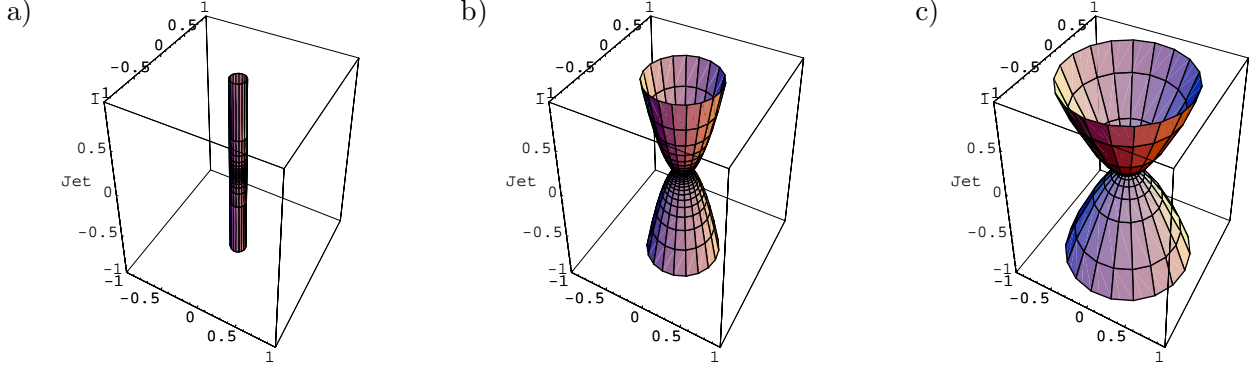


Figure 2: Illustration of the effect of the parameter a in the weight (6) on the shape of the event: a) shape for $a = 1$, b) shape for $a = 0$, c) shape for $a = -1$. The jet axes are in the vertical direction. The radial normalization ($\bar{\varepsilon}Q$) is arbitrary, but the same for all three plots.

3 Factorization and Resummation

3.1 Factorization

Following the procedure developed and extensively discussed in Refs. [8, 9, 10, 11], we first identify the “leading regions”, which can give rise to logarithmic enhancements associated with lines approaching the mass shell. When we sum over all diagrams that have a given final state, the contributions from these leading regions may be factorized into a set of functions, each of which corresponds to one of these generic subdiagrams. The cross section, Eq. (2), then becomes a convolution in $\bar{\varepsilon}$, between functions \bar{J}_c that represent the evolution of the primary partons, and a function \bar{S} that represents coherent soft radiation:

$$\begin{aligned} \frac{d\bar{\sigma}(\varepsilon, \bar{\varepsilon}, a)}{d\varepsilon d\bar{\varepsilon} d\hat{n}_1} &= \frac{d\sigma_0}{d\hat{n}_1} H(Q, \xi_1, \xi_2, \hat{n}_1, \mu) \int d\bar{\varepsilon}_s \bar{S}(\varepsilon, \bar{\varepsilon}_s, a, \mu) \\ &\times \prod_{c=1}^2 \int d\bar{\varepsilon}_{J_c} \bar{J}_c(\bar{\varepsilon}_{J_c}, p_{J_c}, \xi_c, a, \mu) \delta(\bar{\varepsilon} - \bar{\varepsilon}_{J_1} - \bar{\varepsilon}_{J_2} - \bar{\varepsilon}_s), \end{aligned} \quad (7)$$

with p_{J_c} the jet momenta. μ is the factorization scale, which for simplicity we set equal to the renormalization scale. $d\sigma_0/d\hat{n}_1$ is the Born amplitude for the production of a single particle (quark or antiquark) in direction \hat{n}_1 . The ‘short-distance’ function $H(Q, \xi_1, \xi_2, \hat{n}_1, \mu) = 1 + \mathcal{O}(\alpha_s(\mu^2))$, which describes corrections to the hard scattering, is an expansion in α_s with finite coefficients. In Eq. (7) we have suppressed

some arguments of the soft function that are not relevant for the discussion below. The factorized form (7) is illustrated in Fig. 3.

In (7), the “jet functions” \bar{J}_c model radiation collinear to the primary partons, with directions $+\hat{n}_1$ for jet 1, and $-\hat{n}_1$ for jet 2, respectively, and are constructed to be independent of ε , which measures the radiation at wide angles into Ω . The vectors ξ_c are introduced in the factorization of the jet functions from the hard scattering with the help of Ward identities. For further details we refer to [11] and to [6], where the jet functions are related to QCD matrix elements, following [10].

The soft function \bar{S} describes soft radiation at wide angles from the jets, into Ω and $\bar{\Omega}$ alike, and thus depends on both ε and $\bar{\varepsilon}$. From the arguments given in [3, 11], it follows that radiation at wide angles from the primary hard partons decouples from the jets, and can be approximated by an eikonal cross section $\sigma^{(\text{eik})}$, built out of path-ordered exponentials Φ :

$$\Phi_{\beta}^{(f)}(\infty, 0; x) \equiv P e^{-ig \int_0^{\infty} d\lambda \beta \cdot \mathcal{A}^{(f)}(\lambda \beta + x)}, \quad (8)$$

where the β 's are light-like velocities in the directions of the jets. The superscript (f) indicates that the vector potential takes values in representation f, in our case the representation of a quark or an antiquark. An eikonal cross section also contains enhancements for configurations collinear to the jets, which in the factorization (7) are already taken into account in the partonic jet functions. Therefore, the eikonal cross section itself is not a suitable soft function. Rather, to avoid overcounting and to include only soft, but not collinear enhancements, the soft function is defined through the refactorization [2]

$$\begin{aligned} \bar{\sigma}^{(\text{eik})}(\varepsilon, \bar{\varepsilon}_{\text{eik}}, a, \mu) &\equiv \int d\bar{\varepsilon}_s \bar{S}(\varepsilon, \bar{\varepsilon}_s, a, \mu) \\ &\times \prod_{c=1}^2 \int d\bar{\varepsilon}_c \bar{J}_c^{(\text{eik})}(\bar{\varepsilon}_c, a, \mu) \delta(\bar{\varepsilon}_{\text{eik}} - \bar{\varepsilon}_s - \bar{\varepsilon}_1 - \bar{\varepsilon}_2). \end{aligned} \quad (9)$$

In Eq. (9) we have refactorized the eikonal cross section in the same manner as the partonic cross section (7), into eikonal analogs of jet functions, and the same soft function [6]. We have omitted the dependence of the functions in (9) on the eikonal lines β_c and ξ_c for better readability.

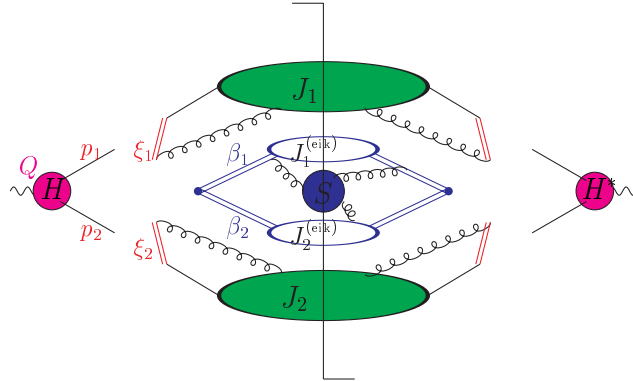


Figure 3: Factorized cross section (7). The vertical line denotes the final state, separating the amplitude (to the left) and the complex conjugate amplitude (to the right).

3.2 Resummation

To disentangle the convolution in (7), we take Laplace moments with respect to $\bar{\varepsilon}$,

$$\begin{aligned} \frac{d\sigma(\varepsilon, \nu, a)}{d\varepsilon d\hat{n}_1} &= \int_0^\infty d\bar{\varepsilon} e^{-\nu \bar{\varepsilon}} \frac{d\bar{\sigma}(\varepsilon, \bar{\varepsilon}, a)}{d\varepsilon d\bar{\varepsilon} d\hat{n}_1} \\ &= \frac{d\sigma_0}{d\hat{n}_1} H(\xi_1, \xi_2, \hat{n}_1, Q) \prod_{c=1}^2 J_c \left(\frac{p_{J_c} \cdot \xi_c}{Q |\xi_c|}, \nu, a, \alpha_s(Q) \right) S(\varepsilon, \nu, a, \alpha_s(Q)) , \end{aligned} \quad (10)$$

where we have exhibited the relevant ξ_c -dependence of J_c [6]. Here and below unbarred quantities are the transforms in $\bar{\varepsilon}$, and barred quantities are untransformed. In Eq. (10) we have set the factorization scale to Q , which avoids large logarithms in the hard function. Large logarithms of ε and ν or $\bar{\varepsilon}$ then occur in the soft and jet functions. In addition, the jets contain potentially large logarithms of $p_{J_c} \cdot \xi_c / (\mu |\xi_c|)$.

The resummation of these logarithms follows from the independence of the physical correlations from the factorization scale and the choice of eikonal factors ξ_c ,

$$\mu \frac{d}{d\mu} \frac{d\sigma(\varepsilon, \nu, a)}{d\varepsilon d\hat{n}_1} = 0, \quad (11)$$

$$\frac{\partial}{\partial \ln(p_{J_c} \cdot \xi_c)} \frac{d\sigma(\varepsilon, \nu, a)}{d\varepsilon d\hat{n}_1} = 0. \quad (12)$$

Following the methods described in Refs. [10, 11, 12], we can use (11) and (12) to derive evolution equations for the jet and soft functions. From this procedure, we derive a resummed expression for the Laplace-transformed correlations [6], which may be written as

$$\begin{aligned} \frac{d\sigma(\varepsilon, \nu, a)}{d\varepsilon d\hat{n}_1} &= \frac{d\sigma_0}{d\hat{n}_1} H(\xi_1, \xi_2, \hat{n}_1, Q) S(\varepsilon \nu, a, \Omega, \alpha_s(\varepsilon Q)) \exp \left[- \int_{\varepsilon Q}^{Q/2} \frac{d\lambda}{\lambda} \gamma_s(\alpha_s(\lambda)) \right] \\ &\times \prod_{c=1}^2 J_c \left(1, 1, a, \alpha_s \left(\frac{Q}{2 \nu^{1/(2-a)}} \right) \right) \exp \left\{ - \int_{\frac{Q}{2 \nu^{1/(2-a)}}}^{Q/2} \frac{d\lambda}{\lambda} \gamma_{J_c}(\alpha_s(\lambda)) \right\} \\ &\times \exp \left\{ - \int_{\frac{Q}{2 \nu^{1/(2-a)}}}^{Q/2} \frac{d\lambda}{\lambda} \left[B_c(a, \alpha_s(\lambda)) + \int_{C_1 \frac{Q^{2-a}}{\nu(2\lambda)^{1-a}}}^{C_2 \lambda} \frac{d\lambda'}{\lambda'} A_c(a, \alpha_s(\lambda')) \right] \right\}, \end{aligned} \quad (13)$$

where we have exhibited the relevant arguments of the soft function. Convenient choices for the scales in the λ' integral are $C_2 = 1$ and $C_1 = \exp[-\gamma_E + (1-a)/2]$. The functions A_c and B_c are associated with the jet functions [10, 12], and the anomalous dimensions γ_s and γ_{J_c} belong to the soft and jet functions, respectively [6, 10]. At lowest order, $A_c = 2C_c(\alpha_s/\pi)$, with $C_c = C_F$ for quarks and C_A for gluons. Other explicit forms are given in [6]. Only the soft function retains dependence on the geometry of the region Ω , as explicitly indicated in (13). Corrections in Eq. (13) of the form $\alpha_s(Q) \ln 1/(\varepsilon \nu)$ occur entirely within the soft function S . For large enough ν and/or $|a|$, at fixed ε , large non-global logarithms reemerge in that function, which may be computed in the eikonal approximation.

So long as we are able to compute corrections in $\alpha_s(Q) \ln 1/(\varepsilon \nu)$ perturbatively, we are free to choose between εQ and Q/ν in any term in (13) that generates single logarithms. Of particular relevance is

the γ_s integral in the first exponential of (13), which reflects the choice of renormalization scale in the soft function S . At higher orders in S , logarithms will arise from gluon emission into angular regions for which the upper limit on energy flow does not match the renormalization scale. Within Ω the upper limit is εQ , and outside, in $\bar{\Omega}$, it is Q/ν . (Recall, there are no collinear enhancements in S .) These logarithms appear multiplied by the size of the angular region from which they arise. When we measure energy flow into a region Ω of small angular extent, it is more convenient to choose a renormalization scale Q/ν , to avoid generating logarithms of $\varepsilon\nu$ multiplied by the size of the larger region $\bar{\Omega}$. Correspondingly, when Ω subtends the bulk of the unit sphere, it is convenient to make the choice of εQ , as in Eq. (13).

4 Results

Eq. (13) resums single logarithms of ε and single and double logarithms of ν . The latter stem from the double integral in the last exponent on the right-hand side. In Figs. 4 and 5 we show some examples of numerical results from (13).

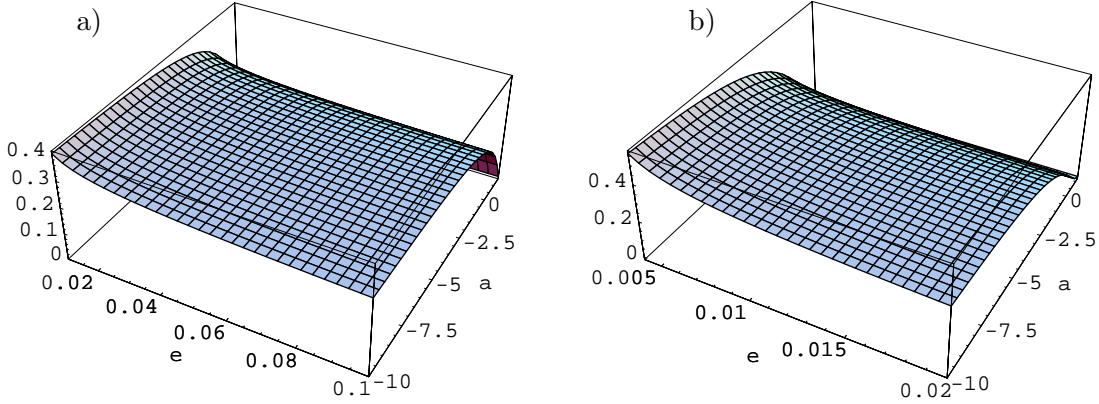


Figure 4: Differential cross section $\frac{\varepsilon d\sigma/(d\varepsilon d\hat{n}_1)}{d\sigma_0/d\hat{n}_1}$, normalized by the lowest order cross section, at $Q = 100$ GeV, as a function of ε and a at fixed ν : a) $\nu = 10$, b) $\nu = 50$. Ω is a slice (ring) centered around the jets, with a width of $\Delta\eta = 2$.

Fig. 4 shows the dependence of the differential cross section (13), multiplied by ε and normalized by the Born cross section, $\frac{\varepsilon d\sigma/(d\varepsilon d\hat{n}_1)}{d\sigma_0/d\hat{n}_1}$, on the measured energy ε and on the parameter a , at fixed ν . We choose the region Ω to be a ring around the jets, centered in their center-of-mass, with a width of $\Delta\eta = 2$. The center-of-mass energy Q is chosen to be 100 GeV. In Fig. 4 a), we plot $\frac{\varepsilon d\sigma/(d\varepsilon d\hat{n}_1)}{d\sigma_0/d\hat{n}_1}$ for $\nu = 10$, in Fig. 4 b) for $\nu = 50$. The cross section falls as $a \rightarrow 2$, where the jets are restricted to be very narrow. Similarly, as ν increases, the radiation into the complementary region $\bar{\Omega}$ is more restricted, as illustrated by the comparison of Figs. 4 a) and b). On the other hand, as $|a|$ increases at fixed ε , the correlations (13) approach a constant value. For $a \rightarrow -\infty$, however, non-global dependence on ε and $|a|$ will emerge from higher order corrections in the soft function.

To illustrate the sensitivity of these results to the flavor of the primary partons, we study the corresponding ratio of the correlation to the cross section for gluon jets produced by a hypothetical

singlet source. Fig. 5 displays the ratio of the differential cross section $d\sigma^q(\varepsilon, a)/(d\varepsilon d\hat{n}_1)$, normalized by the lowest order cross section, to the analogous quantity with gluons as primary partons in the outgoing jets, again at $Q = 100$ GeV. We multiply the ratio by C_A/C_F to compensate for the difference in the normalization of the lowest order soft functions. Gluon jets are wider, and hence are suppressed relative to quark jets as $a \rightarrow 2$ or as ν increases. Figs. 5 a) and b) exhibit this behavior, where we compute the cross section for the same ring around the jets, centered in their center-of-mass, with a width of $\Delta\eta = 2$. Again, Fig. 5 a) is at $\nu = 10$ and b) is at $\nu = 50$. These results suggest sensitivity to the more complex color and flavor flow characteristic of hadronic scattering.

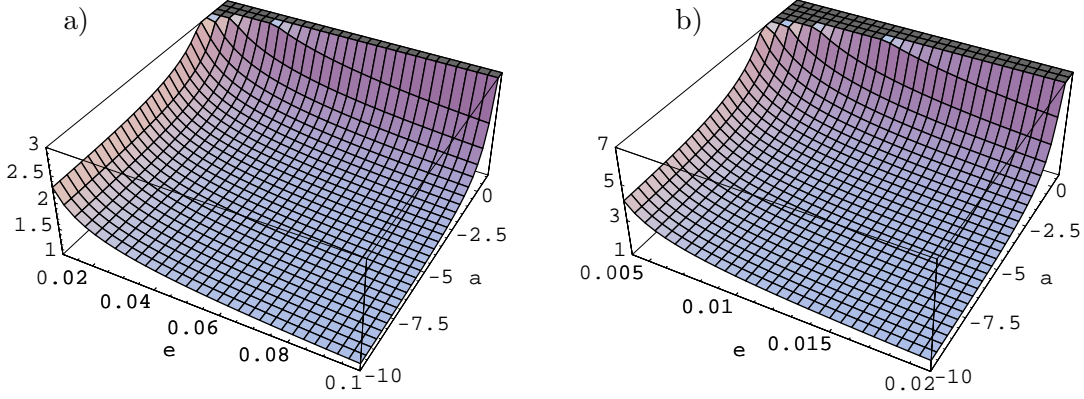


Figure 5: Ratios of differential cross sections for quark to gluon jets $\frac{C_A}{C_F} \left(\frac{\varepsilon d\sigma^q/(d\varepsilon d\hat{n}_1)}{d\sigma_0^q/d\hat{n}_1} \right) \left(\frac{\varepsilon d\sigma^g/(d\varepsilon d\hat{n}_1)}{d\sigma_0^g/d\hat{n}_1} \right)^{-1}$ at $Q = 100$ GeV as a function of ε and a at fixed ν : a) $\nu = 10$, b) $\nu = 50$. Ω , as in Fig. 4, is a slice (ring) centered around the jets, with a width of $\Delta\eta = 2$.

5 Conclusions

We have described a study of interjet energy flow/event shape correlations in e^+e^- dijet events, where all leading effects are treated analytically. By weighting the final state radiation appropriately, our formalism is sensitive mainly to radiation stemming directly from the primary hard scattering. Transforms in a class of weight functions enable us to control the influence of secondary, or non-global, radiation on the energy flow between the jets, and in principle to study correlations between jet structure and energy flow. The study of next-to-leading order and higher corrections in which these effects appear will also be of interest. The application of our formalism to multijet events and to scattering with initial state hadrons is certainly possible, and should shed light on the relationship between color and energy flow in hard scattering processes.

Acknowledgements

We thank Gavin Salam for useful discussions. C.F.B. thanks the National Science Foundation and the sponsors of TH2002 for support at TH2002. This work was also supported in part by the National Science Foundation grant PHY0098527.

References

- [1] Y.L. Dokshitzer, V.A. Khoze, S.I. Troian, *Coherence and physics of QCD jets*, in *Perturbative Quantum Chromodynamics*, ed. A.H. Mueller (World Scientific, Singapore, 1989), p. 241.
J.R. Ellis, V.A. Khoze, W.J. Stirling, Z. Phys. **C 75**, 287 (1997), [hep-ph/9608486].
- [2] N. Kidonakis, G. Oderda, G. Sterman, Nucl. Phys. **B 531**, 365 (1998), [hep-ph/9803241].
- [3] C.F. Berger, T. Kúcs, G. Sterman, Phys. Rev. **D 65**, 094031 (2002), [hep-ph/0110004].
- [4] J. Huston, V. Tano, in summary report for the Workshop on Physics at TeV Colliders, Les Houches, France, 1999, [hep-ph/0005114].
CDF Collaboration (Rick D. Field for the collaboration), contributed to APS/DPF /DPB Summer Study on the Future of Particle Physics (Snowmass 2001), Snowmass, Colorado, 2001, [hep-ph/0201192].
- [5] M. Dasgupta, G.P. Salam, Phys. Lett. **B 512**, 323 (2001), [hep-ph/0104277].
M. Dasgupta, G.P. Salam, JHEP **0203**, 017 (2002), [hep-ph/0203009].
M. Dasgupta, G.P. Salam, JHEP **0208**, 032 (2002), [hep-ph/0208073].
- [6] C.F. Berger, T. Kúcs, G. Sterman, in preparation.
- [7] A. Banfi, G. Marchesini, Y.L. Dokshitzer, G. Zanderighi, JHEP **0007**, 001 (2000), [hep-ph/0004027].
S.J. Burby, N. Glover, JHEP **0104**, 029 (2001), [hep-ph/0101226].
A. Banfi, G. Marchesini, G. Smye, JHEP **0208**, 006 (2002), [hep-ph/0206076].
R.B. Appleby, M.H. Seymour, hep-ph/0211426.
- [8] G. Sterman, Phys. Rev. **D 17**, 2773 (1978).
- [9] J.C. Collins, G. Sterman, Nucl. Phys. **B 185**, 172 (1981).
- [10] J.C. Collins, D.E. Soper, Nucl. Phys. **B 193**, 381 (1981).
- [11] J.C. Collins, D.E. Soper, G. Sterman, *Factorization of hard processes in QCD*, in *Perturbative Quantum Chromodynamics*, ed. A.H. Mueller (World Scientific, Singapore, 1989), p. 1.
- [12] H. Contopanagos, E. Laenen, G. Sterman, Nucl. Phys. **B 484**, 303 (1997), [hep-ph/9604313].